

# ITALSAT Ka, Q and V band Cross polar discrimination statistics measured in Spino d'Adda, Italy

Eric Regonesi\*, Carlo Riva\*<sup>†</sup>, Lorenzo Luini\*<sup>†</sup>, Antonio Martellucci<sup>‡</sup>

\* DEIB: Politecnico di Milano, Milan, Italy, eric.regonesi@polimi.it

<sup>†</sup> IEIIT: Consiglio Nazionale delle Ricerche (CNR), Milan, Italy

<sup>‡</sup> European Space Agency (ESA), Noordwijk, The Netherlands

**Abstract**—Cross polar discrimination (XPD) is a widespread parameter used to measure the disturbance introduced on electromagnetic signals by the loss of polarisation, when dual polarisation links are employed. Rain precipitations and ice clouds contribute to the increase of XPD in the atmosphere. The current ITU-R Recommendation P.618 links the prediction of the XPD to the excess attenuation probability of a specific site. The statistical analysis of the XPD reported in this contribution is a basic step towards an improved model for next generation dual polarisation links design.

**Index Terms**—depolarisation, cross polar discrimination, propagation, measurements.

## I. INTRODUCTION

Dual polarisation techniques are often used to increase the capacity of terrestrial and satellite radio communication systems. This approach comes with an increased complexity in the transmission and reception chains and some additional impairments on the available signals. The presence of non-spherical atmospheric hydrometeors (like rain, ice and melting particles) in the troposphere can cause the increase in the noise due to the transfer of energy between orthogonal polarisation states that creates crosstalk between the copolar and crosspolar radio channels [1][2]. Such problems have raised the necessity of propagation campaigns to better characterize the loss of polarisation caused by the atmosphere. Among them, ITALSAT/F1 experiment started in 1992, with three ground stations located in Italy: Torino, Pomezia (Rome) and Spino d'Adda (Milan). The experiment was characterized by the transmission of beacons at Ka, Q and V bands [3]. This contribution presents the cumulative statistics of the cross polar discrimination (XPD), for the site of Spino d'Adda. In addition to the ones presented in [4] at V band in circular polarisation, we introduce here the XPD statistics at Ka and Q bands. We also include the XPD statistics at V band, but in linear polarisation.

## II. THE CROSS POLAR DISCRIMINATION

Let us consider the transmission of an electromagnetic wave through a generic medium. The input electric field is related

to the output electric field by the 2-by-2 transfer matrix [4] given in (1):

$$\begin{bmatrix} E_{1,out} \\ E_{2,out} \end{bmatrix} = \begin{bmatrix} T_{11} & T_{12} \\ T_{21} & T_{22} \end{bmatrix} \begin{bmatrix} E_{1,in} \\ E_{2,in} \end{bmatrix} \quad (1)$$

Notice here that the subscripts 1,2 refer to two generic orthogonal components, which might be polarized either as linear (in this work) or circular. The cross polar discrimination, a parameter widely used to measure the depolarisation, is defined as (2)

$$XPD_{ij} = 20 \log_{10} |\delta_{ij}| \quad (2)$$

where  $\delta_{ij}$  ( $i, j = 1, 2; i \neq j$ ) represents the generic cross polar ratio (3):

$$\delta_{ij} = \frac{T_{ij}}{T_{jj}} \quad (3)$$

The XPD has been found to be an important parameter when describing dual polarisation satellite communications systems, since it is related to the differential attenuation and phase shift between the two orthogonal electromagnetic components. A good knowledge of the XPD is fundamental to build prediction models, whose physical basis is strongly encouraged by the International Telecommunication Union [5]. One of the foreseen models, compliant with the need of a physical basis, relies on the usage of the quasi-physical parameters [4], *i.e.* the anisotropy and the canting angle. The actual ITU-R P.618 Recommendation [6] provides XPD predictions as a function of the site specific excess attenuation probability (also known as co-polar attenuation, CPA), through an empirical model. The ice clouds effect is taken in due account with an additive (in decibels) correction factor.

## III. DATABASE

The ITALSAT satellite (13° longitude E) transmitted beacons at Ka, Q and V bands. The 18.7 GHz signal was vertically polarized. At the frequency of 39.6 GHz, it transmitted a circular right handed polarisation. Finally, the beacon at 49.5 GHz was switched between two linear orthogonal polarisations (vertical and horizontal), to allow characterizing the full polarisation transfer matrix. The corresponding ground station of Spino d'Adda was equipped with a 3.5 m diameter antenna,

at an elevation of  $37.7^\circ$ . The antenna XPD is equal to  $-30$  dB [4].

The database of measurements used to assess the statistics of the co-polar attenuation and cross polar discrimination contains 131 events, recorded between 1992 and 2000. The ground station recorded the amplitude and the phase of both the co-polar and cross polar channels signals.

#### A. Pre-processing

For the signals originally transmitted with a single polarisation, we extracted first the signal power level and the complex cross polar ratio. Both these time series underwent a two stages pre-processing phase, event based: first, the clear sky effect was removed [7]; secondly, an adaptive filtering on the measured level of the XPD was applied [4]. The received power was expressed in logarithmic units whereas the cross polar ratio was in linear units. We refer hereafter to both the quantities as the "reference signal", since they were subject to the same processing. The reference signal in clear sky conditions, which includes the contribution of the transmission systems, was obtained by averaging its value in the minutes preceding and following the event. By means of a vector correction procedure [8], the reference signal was linearly interpolated in time and subtracted from the recorded signals. An adaptive filtering was then applied, based on the reference extracted level of the cross polar discrimination. The higher was the XPD, the shorter was the length of the low pass filter window, to maintain a good compromise between time details and noise removal. The filtering phase also removed the effect of scintillations, whose cutoff frequency was set to  $f_{cut} = 0.025$  Hz [9]. The data at 39.6 GHz required a longer window (in time), due to the higher noise floor inferred from a spectral analysis. For each event, the two time series of CPA and XPD thus obtained were saved and used as input of the post-processing phase.

The signals transmitted with a double polarisation were corrected of the system effects on the transfer matrix. The correction procedure is the one adopted in [4].

#### B. Post-processing

In the post-processing phase, we removed non physical behaviours of the series. For instance, an entire event on 1993/5/2 was completely removed because of errors in the receiving chain. Finally, the data of all the events were combined to calculate the overall deciles of the XPD values conditioned to the CPA levels and the complementary cumulative distribution functions (CCDF) of the XPD, conditioned to different CPA ranges. Taking into account the intrinsic limitations of the measurement system and of the correction procedures, we mainly took the heed of the data presenting a XPD value higher than  $-60$  dB and a CPA value lower than  $30$  dB. The additional limitation given by both the number of samples and the maximum excess attenuation recorded further restricted the considered data at Ka band to the samples with a CPA lower than  $15$  dB.

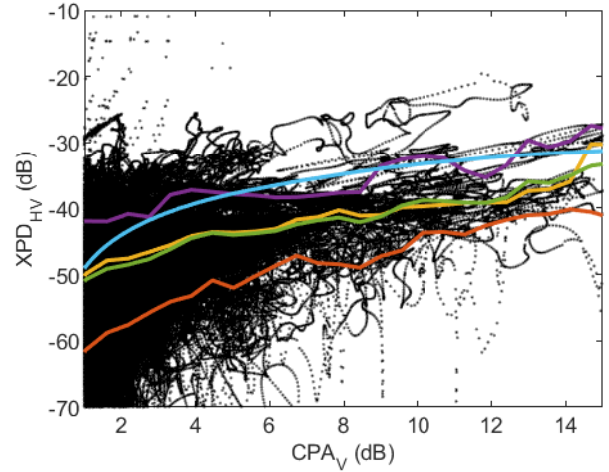


Fig. 1. Scatterplot of  $XPD_{HV}$  versus  $CPA_V$  for the site of Spino d'Adda, at 18.7 GHz. Red, yellow and purple curves are the 10, 50 and 90 percentiles of XPD conditioned to CPA values. The green curve represents the mean whereas the cyan line is the ITU-R P.618-13 model prediction, for the site specific excess attenuation.

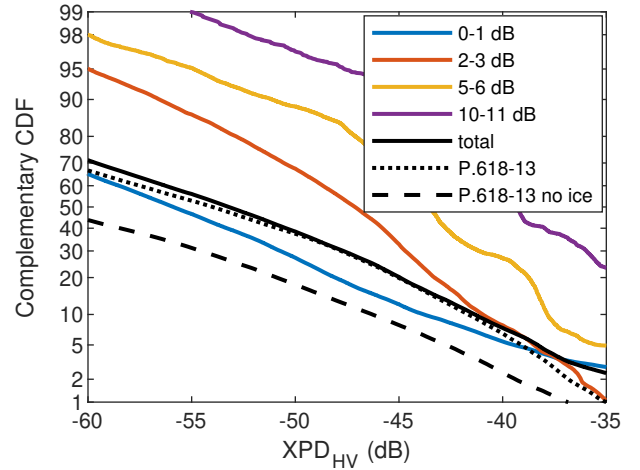


Fig. 2. Complementary cumulative distribution functions (CCDF) of the XPD for the Spino d'Adda site at 18.7 GHz, for the selected excess attenuation ranges (coloured curves) and the entire excess attenuation (black curves). The dotted and dashed curves represent the ITU-R P.618-13 CCDF predictions, respectively including and neglecting the effect of the ice.

## IV. RESULTS

#### A. XPD statistics analysis at Ka band

Figure 1 shows the cumulative scatterplot of the XPD for the signal at 18.7 GHz along with the correspondent vertically polarized CPA. The mean (green) and the 10, 50 and 90 percentiles (red, yellow and purple, respectively) have been included as well in the graph. The functional form used by ITU-R Recommendation P.618-13 to predict equiprobable values of XPD from CPA values is also plotted (cyan). We can notice how this functional form corresponds roughly to the 90% decile of the measurements in Spino d'Adda, except

for low levels of the excess attenuation, where the ITU-R curve tends to the 50% percentile of the measurements. The percentiles and the mean values also suggest a linear shape for the XPD prediction model.

Figure 2 shows the CCDFs of the cross polar discrimination, for selected intervals of CPA and for the entire excess attenuation range, in a normal distribution chart. A normal distribution appears to be applicable for low attenuation values and for the total distribution. For the distribution in presence of higher attenuation (*i.e.* 5 to 11 dB) the statistics could be less stable at lower XPD values because of the lower number of samples (as also seen in Figure 1). In these cases we can use the mean and standard deviation to model the data using a normal, as the approach presented in [4]. The CCDF of the equiprobable CPA-based XPD predictions by ITU-R is included as well, both including and neglecting (dotted and dashed black curves, respectively) the empirical ice crystal dependent term in [6]. At Ka band, the total site CCDF and the predicted one fairly agree for all the probability ranges.

### B. XPD statistics analysis at Q band

Figure 3 reports the cumulative cross polar discrimination scatterplot for the right-hand circularly polarized signal transmitted at 39.6 GHz. It is clearly visible that the XPD values reached for high CPAs at this frequency are pretty high - as expected theoretically for the depolarisation of circular polarisations -, even higher than the ones recorded at 49.5 GHz (see Figure 19 of [4] for reference). The mean and the 90% and 50% percentiles shown on Figure 3 follow a linear trend with the increase in the excess attenuation. In this case the functional form of the ITU-R Recommendation P.618-13 for the prediction of the equiprobable distribution of XPD, appears to be representative of the 50% percentile of measurements for attenuations ranging between 5 and 15 dB, whilst it represents a lower fraction of data for lower or higher attenuation. This behaviour could be explained by separate microphysical phenomena occurring at low and high attenuations (e.g. ice in absence of rain and level of alignment, and rain drop size distribution in presence of heavy precipitation).

As we did for the frequency of 18.7 GHz, we have extracted the CCDFs of the circularly polarized XPD at 39.6 GHz (Figure 4). In some cases it seems possible to approximate the distributions as Gaussian, both for the entire and the selected ranges of CPA. By comparing total distribution of measurements it can be seen that the ITU-R model underestimates XPD values of about 5 dB or more for all the probability values.

### C. XPD statistics analysis at V band

For completeness, we repeated the same processing for the linearly polarized data at the frequency of 49.5 GHz. The scatterplot of the XPD versus the CPA and the CCDFs of the XPD are reported in Figures 5 and 6, respectively. Differently from Figures 19 and 20 reported in [4], we have analysed the depolarisation of the linear polarisation at 49.5 GHz to be congruent with the results for the signal 18.7

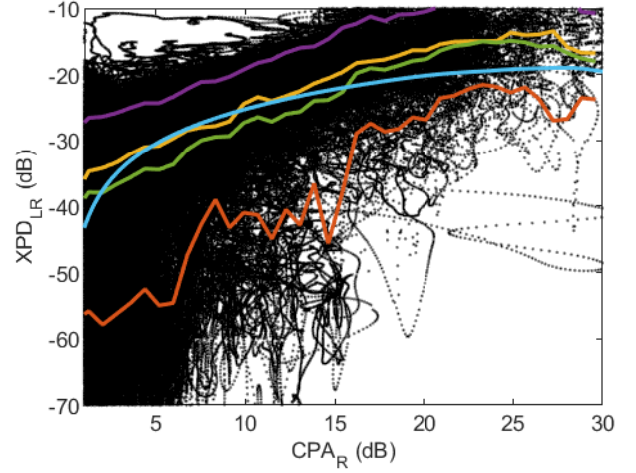


Fig. 3. Scatterplot of  $XPD_{LR}$  versus  $CPA_R$  for the site of Spino d'Adda, at 39.6 GHz. Red, yellow and purple curves are the 10, 50 and 90 percentiles of XPD conditioned to CPA values. The green curve represents the mean whereas the cyan line is the ITU-R P.618-13 model prediction, for the site specific excess attenuation.

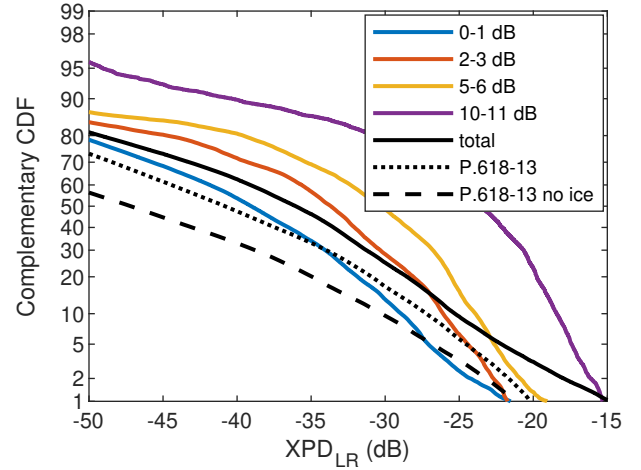


Fig. 4. Complementary cumulative distribution functions (CCDF) of the XPD for the Spino d'Adda site at 39.6 GHz, for the selected excess attenuation ranges (coloured curves) and the entire excess attenuation (black curve). The dotted and dashed curves represent the ITU-R P.618-13 CCDF predictions, respectively including and neglecting the effect of the ice.

GHz reported in Figures 1 and 2. Also in this case, we can notice that the functional form of ITU-R P.618 model for the prediction of equiprobable XPD values appears to be in agreement with a lower fraction of the measurements (between 50 and 10%). The mean tends to be linear with the increase of the excess attenuation. The cumulative distribution functions confirm the hypothesis of Gaussian modeling suggested in [4]. As observed at Q band, the ITU-R model underestimates XPD of about 10 dB or more for all probability ranges.

We have found that, when frequency and polarisation change, the ITU-R functional behaviour corresponds to different deciles of the measured joint distribution of XPD-CPA.

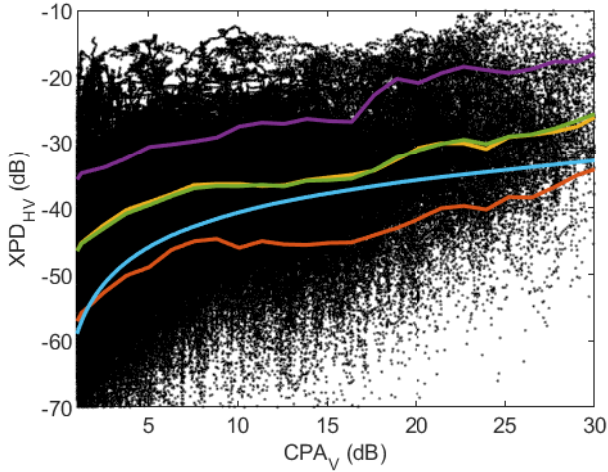


Fig. 5. Scatterplot of  $XPD_{HV}$  versus  $CPA_V$  for the site of Spino d'Adda, at 49.5 GHz. Red, yellow and purple curves are the 10, 50 and 90 percentiles of XPD conditioned to CPA values. The green curve represents the mean whereas the cyan line is the ITU-R P.618-13 model prediction, for the site specific excess attenuation.

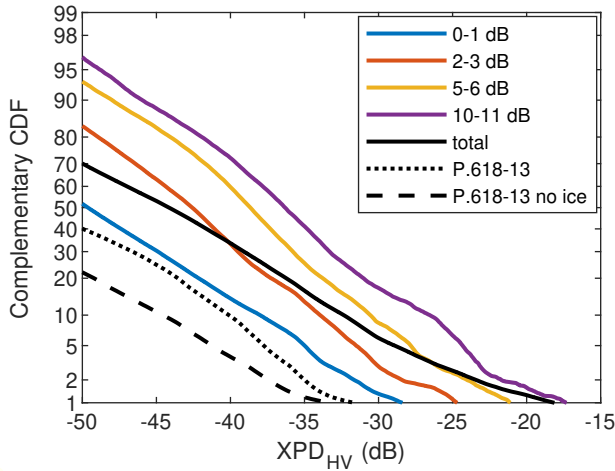


Fig. 6. Complementary cumulative distribution functions (CCDF) of the XPD for the Spino d'Adda site at 49.5 GHz, for the selected excess attenuation ranges (coloured curves) and the entire excess attenuation (black curve). The dotted and dashed curves represent the ITU-R P.618-13 CCDF predictions, respectively including and neglecting the effect of the ice.

This is an indication that the underlying ITU-R assumptions are more or less representative in the different configurations. A full assessment can be done only by using the transfer matrix and the quasi-physical parameters, but these are aspects that a future model shall be able to reproduce.

## V. CONCLUSION

We have analyzed the ITALSAT/F1 data for all the frequencies of the transmitted beacons, for the site of Spino d'Adda (Milan). We have defined a consistent method for depolarisation data processing to remove the noise and to extract the variables of interest, *i.e.* the XPD and the CPA.

We have shown the relation between the depolarisation and the excess attenuation by reporting on the scatterplots the statistics of the XPD (10, 50 and 90 percentiles plus the mean, conditioned to the CPA) and the prediction of the XPD given by the in force ITU-R P.618 Recommendation model.

We have seen that the Recommendation suggests a logarithmic model, which in a number of cases is in contrast with the linear behaviour of the data statistics. Furthermore, the functional proposed by ITU-R P.618-13 for the prediction of equiprobable XPD-CPA values, represents different fractions of the observations for the various frequencies and polarisations (*i.e.* the 90% decile conditioned to attenuation for vertical polarisation at 19.7 GHz, the 50% decile for circular polarisation at 39.6 GHz and less than 50% for vertical polarisation at 49.5 GHz). A specific analysis based on the physical properties of the depolarising medium could be used to model this behaviour.

The computed CCDFs of the site specific XPDs, confirm that they can be modeled as a Gaussian function, thus only focusing on the study of the mean and the standard deviation, as did in the analysis in [4]. The results presented encourage to search for a linear model for the joint rain and ice XPD predictions, given the knowledge of the excess attenuation. Such a model must be frequency dependent, to cope with the slopes of the observed XPD mean and median values.

## REFERENCES

- [1] D. Cox, "Depolarization of radio waves by atmospheric hydrometeors in earth-space paths: A review," *Radio science*, vol. 16, no. 05, pp. 781–812, 1981.
- [2] T. Oguchi, "Electromagnetic wave propagation and scattering in rain and other hydrometeors," *Proceedings of the IEEE*, vol. 71, no. 9, pp. 1029–1078, 1983.
- [3] Agenzia Spaziale Italiana, "Italsat propagation experiment: Users' guide," 1992.
- [4] A. Paraboni, A. Martellucci, C. Capsoni, and C. G. Riva, "The physical basis of atmospheric depolarization in slant paths in the v band: theory, italsat experiment and models," *IEEE Transactions on Antennas and Propagation*, vol. 59, no. 11, pp. 4301–4314, 2011.
- [5] International Telecommunication Union, "Acquisition, presentation and analysis of data in studies of radiowave propagation," *ITU Rec. ITU-R P.311-14*, 2013.
- [6] —, "Propagation data and prediction methods required for the design of earth-space telecommunication systems," *ITU Rec. ITU-R P.618-13*, 2017.
- [7] A. Martellucci, A. Paraboni, and M. Filipponi, "Measurements and modelling of rain and ice depolarization on spatial links in the ka and v frequency bands," in *AP2000 Millenium Conference on Antennas and Propagation*, 2000, pp. 1–4.
- [8] P. van de Berg, G. Brussaard, and J. Dijk, "On the accuracy of radiowave propagation measurements," in *1990 20th European Microwave Conference*, vol. 1. IEEE, 1990, pp. 656–661.
- [9] E. Matricciani, M. Mauri, and C. Riva, "Relationship between scintillation and rain attenuation at 19.77 ghz," *Radio Science*, vol. 31, no. 02, pp. 273–279, 1996.